ISBN: 978-3-95450-214-1 ISSN: 2673-5490 doi:10.18429/JACoW-IPAC2021-WEPAB330

# A MULTIRANGE LOW NOISE TRANSIMPEDANCE AMPLIFIER FOR SIRIUS BEAMLINES

L. Y. Tanio†, F. H. Cardoso, M. M. Donatti,
Brazilian Synchrotron Light Laboratory (LNLS) Campinas, Brazil

*Abstract*

In a typical synchrotron beamline, the interaction of photon beams with different materials generates free electric charges in devices such as ionization chambers, photodiodes, or even isolated metallic structures (e.g., blades, blocks, foils, wires). These free charges can be measured as electric current to diagnose the photon beam intensity, profile, position, or stability. Sirius, the new 3 GeV fourth-generation Brazilian light source, may accommodate up to 38 beamlines, which combined will make use of hundreds of instruments to measure such low-intensity signals. This work reports on the design and test results of a transimpedance amplifier developed for low current measurements at Sirius' beamlines. The device presents low noise, high accuracy, and good temperature stability providing 5 selectable ranges (from 500 pA to 7.3 mA) to measure bipolar currents achieving femtoampere resolution under certain conditions. Considering low bandwidth applications, the results suggest noise performance comparable to commercial bench instruments. Additionally, the project definitions and plans for the development of a family of low current ammeters will be discussed.

## INTRODUCTION

The construction of a new fourth-generation synchrotron brings the challenge in many engineering areas. There are situations in which the solutions or the devices available in the market are expensive or not suitable due to aspects such as the size, performance, update rate, communication interface, or even because of incompatible infrastructure. For those reasons, the electronic instrumentation group, in the Brazilian Synchrotron Light Laboratory (LNLS/CNPEM), has designed a low noise current-to-voltage amplifier.

There are well-known topologies [1] that are suitable for low current measurements, such as charge integrators, shunt resistors and the classic transimpedance amplifiers. All of them convert the input current/charge to a proportional voltage using operational amplifiers and accompanying circuits. Considering the pros and cons characteristics we have designed an ammeter based on a transimpedance of each topology (I – V converter). With a small form factor, the designed circuit has extremely low input bias current, minimal input voltage burden and very low noise, becoming a suitable solution for a wide range of applications in synchrotron experimental stations and their diversity of experiments.

† lucas.tanio@lnls.br

## TRANSIMPEDANCE AMPLIFIER

The transimpedance amplifier is a current to voltage (I-V) converter that makes use of an operational amplifier and a feedback resistor (RF) [2] also known as transimpedance gain. A feedback capacitor (CF) is placed in parallel with the resistor to stabilize the circuit and limit the bandwidth [3]. The output voltage and the cutoff frequency of an ideal transimpedance amplifier are shown in Eq. (1) and Eq. (2) and respectively.

$$V_{out} = -I_{in} R_F \tag{1}$$

$$f_c = \frac{1}{2\pi R_F C_F} \tag{2}$$

### *Noise Analysis and Circuit Stability*

The noise analysis of the classic transimpedance amplifier considers two major noise sources [4, 5]: the operational amplifier noise and the feedback resistor's thermal noise. For a more general analysis, in this work, the noise discussion uses the noise density terms, instead of the overall noise.

The total output noise voltage density is given by Eq. (3), where $e_{nv}$ and $e_{ni}$ are, respectively, the operational amplifier voltage and current noise contribution referred to the output voltage noise density and $e_{n\_Rf}$ is noise density from the feedback resistor.

$$e_{noise} = \sqrt{e_{nv}^2 + e_{ni}^2 + e_{n\_Rf}^2} \tag{3}$$

The operational amplifier input noise densities values can be found in the datasheet, but they must be referenced to the output: the input voltage noise density value must be multiplied by the voltage gain network (feedback resistor and input resistance), and the input current noise density by the transimpedance gain. The noise density from the feedback resistor is modelled using Johnson's noise density equation [Eq. (4)], where k is the Boltzmann constant, T is the absolute temperature in Kelvin, and R is the resistance value.

$$e_n = \sqrt{4kTR} \tag{4}$$

A way to analyze the stability in transimpedance amplifiers is based on phase margin estimation. According to [6], there is a figure of merit applicable to minimum-phase circuits, the rate of closure (ROC), that helps to estimate the circuit's phase margin that is given by Eq. (5). The ROC is the difference between the noise gain slope in dB/dec and the operational amplifier open-loop gain also in dB/dec at the cross-over frequency.

$$pm = 180° - 4.5\, xROC \tag{5}$$

ISBN: 978-3-95450-214-1 ISSN: 2673-5490 doi:10.18429/JACoW-IPAC2021-WEPAB330

From Eq. (5), considering 45° the minimum phase margin to avoid circuit instabilities, it is possible to determine the minimum feedback capacitor needed to stabilize the circuit, given by Eq. (6).

$$C_f > \frac{1}{4\pi R_f f_{gbw}}\left(1+\sqrt{1+8\pi R_f f_{gbw} C_{in}}\right) \quad (6)$$

## DESIGN DETAILS

### *Circuit Implementation*

To measure extremely low-intensity currents, the chosen operational amplifier meets several parameters such as input bias current, voltage and current noise density, input offset voltage and low offset drift [7].

The wide dynamic range for current measurements, from few femtoamperes to units of milliamperes, is guaranteed using the classical multirange transimpedance amplifier circuit [8]. For this application, we used high insulation reed relays to select different gain resistors on the amplifier stage. Due to the PCB physical space limitation, there are five selectable transimpedance gains available. A simple onboard digital circuit was implemented to drive the relays.

Concerning transimpedance gain, the circuit was implemented using high precision and low temperature coefficient SMD resistor (1206, ±0.1 %, ±25 ppm/ºC) except for the highest gain scale (1206, ±10 %, ±250 ppm/ºC) since it is the only SMD resistor available at the market to perform the desirable transimpedance gain. To limit the circuit bandwidth and provide circuit stability, the feedback capacitors have been chosen considering two intrinsic properties: good thermic stability and low leakage [9]. Mica capacitors were used only for the two most sensible gains and common NP0 ceramic capacitors for other ranges.

Table 1: Feedback Resistor, Sensitivity, Full-Scale Current, Feedback Capacitor, Capacitor Type, and Theoretical Cutoff Frequency

| $R_F$ (Ω) | Sensitivity (A/V) | Full-scale (A) | $C_F$ (nF) | $f_c$ (kHz) |
|---|---|---|---|---|
| 10 G | 100 p | 500 p | 0.001 | 0.016 |
| 100 M | 10 n | 50 n | 0.001 | 1.6 |
| 1 M | 1 µ | 5 µ | 0.1 | 1.6 |
| 10 k | 100 µ | 500 µ | 10 | 1.6 |
| 680 | 1.4 m | 7 m | 220 | 1 |

The capacitor values were decided considering a project constraint to have the same bandwidth for every transimpedance gain, unless for the most sensible scale (100 pA/V), that is limited for much lower cutoff frequency.

Table 1 summarizes all ranges characteristics considering a ±5V output voltage excursion.

To supply the amplifier, an external ultra-low noise power supply (ULPNS) was designed. This device is based on switching DC-DC converters and low noise regulation stages and can supply up to four current amplifiers. Despite this, the amplifier board still has an additional bipolar low noise voltage regulator to provide extra PSSR (Power Supply Rejection Ratio).

### *Low Noise Techniques*

The PCB was designed to guarantee an extremely low current leakage path from the input connector to the input pin using guarding and shielding techniques [1, 10]. The board design comprises the use of solutions such: guard ring tracks, planes and metallic shielding driven by a guard buffer circuit, combined with PCB cut-outs and solder mask removal from sensitive regions.

To reduce overall noise, switching noise coupling from the digital circuitry on the analog signals or ground loop issues, the PCB layout was made using split ground planes [11] with a well-planned current return path. Via fences were positioned to protect sensitive signals and decoupling capacitors were largely used. Figure 1 shows the assembled board.

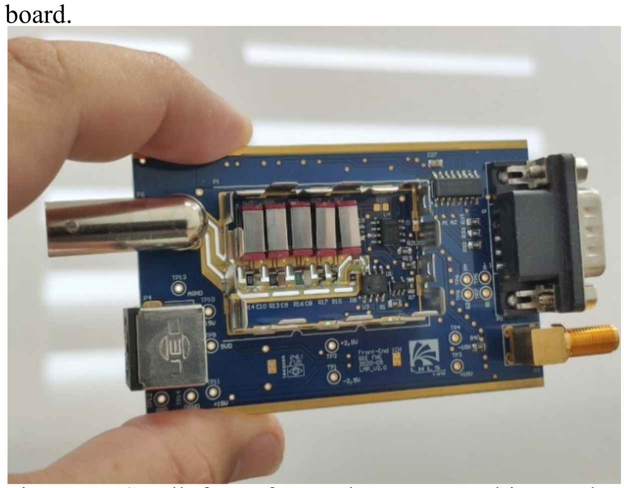

Figure 1: Small form factor, low-cost, multirange low noise transimpedance amplifier.

### *Cleaning Process*

After the PCB soldering, impurities such as solder flux and body oil may be present. From empirical observations, these contaminants may cause unwanted offset voltages that hinder low current measurements (sub nanoampere range). For this reason, a cleaning process was established. The procedure comprises 30 minutes of ultrasonic bath with isopropyl alcohol (IPA) 99% followed by an oven drying period (125ºC – 30 min). From our observations, the overall output offset voltage can be reduced, on average, three orders of magnitude, reaching microvolt levels. Additionally, a silica gel packet is also positioned inside the electronics enclosure to act as a drying agent.

## RESULTS

The characterization setup uses a CompactRIO hardware with 24 bits NI-9239 ADC module [12] and a Keithley 6221 precision current source [13] to evaluate three figures of merit: gain, bandwidth, and noise spectral density.

From the gain characterization, in the four lower gain ranges, the maximum gain error was 0.15%. While in the higher gain scale (pA range), the maximum gain error was

ISBN: 978-3-95450-214-1 ISSN: 2673-5490 doi:10.18429/JACoW-IPAC2021-WEPAB330

less than 6%. These gain errors can be calibrated and agree with the feedback resistor's tolerance and current source error.

The bandwidth analysis presented lower cutoff frequency values than expected in Eq. (2). This can be explained by parasitic capacitances in the circuit. For µA and mA ranges, the average error is closer to the capacitor and resistor combined tolerances.

Table 2 shows the expected theoretical noise spectral density for designed ranges. These values were calculated using Eq. (3) and Eq. (4), as explained in the "*Noise Analysis and Circuit Stability*" section.

Table 2: Theoretical Noise Spectral Density Expected for Different Ranges

| Full Scale | Current NSD | Voltage NSD |
|---|---|---|
| 500 pA | 1.3 fA/√Hz | 12.9 uV/√Hz |
| 50 nA | 13.5 fA/√Hz | 1.3 uV/√Hz |
| 5 µA | 248.3 fA/√Hz | 248.3 nV/√Hz |
| 500 µA | 21.3 pA/√Hz | 212.7 nV/√Hz |
| 7.3 mA | 312.3 pA/√Hz | 212.3 nV/√Hz |

To perform the noise analysis, an open shielded cap connector is placed at the amplifier's input. The input-referred current noise spectral density can be calculated by Welch's Power Spectrum Density method [14]. Figure 2 shows the noise spectral density for the two most sensitive ranges using data acquired at 50 kS/s.

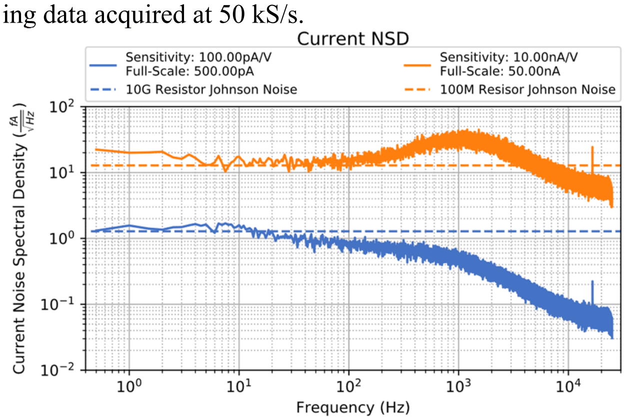


Figure 2: Current noise spectral density of the two most sensitive ranges.

Although the results presented in Fig. 2 agree with the estimated values (Table 2), the experimental setup limits higher ranges noise measurements, once the NI-9239 voltage noise density is about 443nV/√ Hz, greater than expected for the picoammeter design.

To evaluate the in-house transimpedance amplifier performance, we compared its noise spectral density with two commercial bench instruments: the Stanford SR570 [15] and Keysight B2981 [16]. The NSD in the 100 pA/V sensitivity, can be seen in Fig. 3. Unfortunately, the instruments could not be tested using the same bandwidth: the SR570 was configured to 100 Hz, the bandwidth of the LNLS amplifier was fixed at 16 Hz and the B2981 analog output cannot be configured but has less than 1 Hz BW.

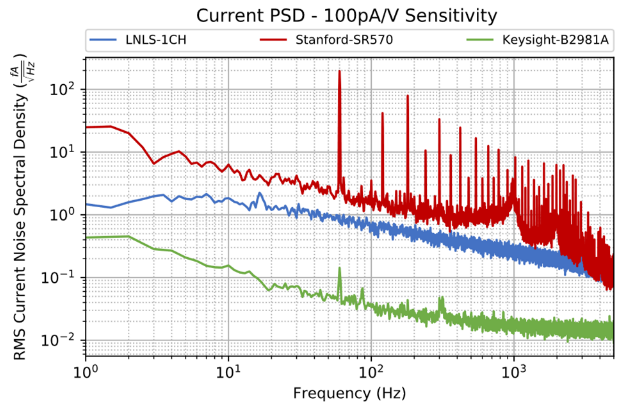


Figure 3: Noise density comparison.

The LNLS amplifier has a noise level in the same order of magnitude as the commercial instruments, and it has an effective immunity to mains frequency noise coupling.

## CONCLUSIONS

We have designed a low-cost multirange low noise transimpedance amplifier. With a small form factor, the amplifier is suitable to measure currents ranging from picoampere to milliampere. Given the large number of devices required for low current monitoring at Sirius, the in-house development showed to be a more cost-effective solution. For the first fourteen beamlines, 75 units were produced.

Several error sources can have serious impacts on low current measurement electronics. The right component choice and all the strategies adopted to make a proper guarding, shielding and PCB layout showed to be effective to reduce static and dynamic errors. The cleaning process is an indispensable procedure to reduce output offset voltage for the most sensitive range.

The deviation found in gain and bandwidth specification is within the component's tolerance and can be calibrated or does not impact the beamline's applications.

In low bandwidth applications, the noise performance is on the same order of magnitude of commercial bench equipment. An appropriate test setup, using a higher resolution ADC, is under evaluation for an improved NSD characterization.

## FUTURE PLANS

Finally, to fulfill the Sirius beamlines applications other devices must be developed in a near future.

Beam position monitors or slit systems need four simultaneous monitoring channels and thus, it will be necessary to use a digital picoammeter with four amplifier stages followed by integrated ADC´s and an embedded microcontroller. The device must provide ethernet interface and real-time signal processing capabilities.

Furthermore, for high dynamic range measurements, sensitive to gain changes, a low noise single scale logarithmic amplifier must be developed.

ISBN: 978-3-95450-214-1 ISSN: 2673-5490 doi:10.18429/JACoW-IPAC2021-WEPAB330



## REFERENCES


[1] Keithley Instruments, *Low Level Measurements Handbook-Precision DC current, voltage and resistance measurements*, Cleveland, OH, USA: Keithley Instruments, 2014.

[2] B. Pease, What's All This Transimpedance Amplifier Stuff, Anyhow? (Part 1), Jan. 2001, https://www.electronicdesign.com/technologies/analog/article/21801223/whats-all-this-transimpedance-amplifier-stuff-anyhow-part-1

[3] A. Bhat, "Stabilize Transimpedance Amplifier Circuit Design," Maxim Integrated, San Jose, California, USA, Rep. APP5129, Feb. 2012

[4] Texas Instruments, "Noise Analysis of FET Transimpedance Amplifier," Texas Instruments, Tucson, AZ, USA, Rep. SBOA060, Feb. 1994.

[5] M. Demirtaş, M. A. Erişmiş, and S. Güneş, "Analysis and design of a transimpedance amplifier based front-end circuit for capacitance measurements," *SN Applied Sciences*, vol. 2, no. 2, Jan. 2020. doi: 10.1007/s42452-020-2104-x

[6] D. S. Franco, Phase Margin Estimation Using the Rate-of-Closure - Technical Articles, Mar. 2019, https://www.allaboutcircuits.com/technical-articles/phase-margin-estimation-using-the-rate-of-closure/ .

[7] B. Trump, *The Signal e-book: A compendium of blog posts on op amp design topics,* Online: Texas Instruments, 2017. http://www.ti.com/lit/slyt701.

[8] L. Orozco, "Programmable-Gain Transimpedance Amplifiers Maximize Dynamic Range in Spectroscopy Systems," *Analog Dialogue*, vol. 47, no. 2, pp. 47-05, May 2013.

[9] Analog Devices Inc., "Passive Components," in *Linear Circuit Design Handbook*, Ed. H. Zumbahlen, Newnes/Elsevier, Feb. 2008, pp. 10.1-10.28. doi:10.1016/b978-0-7506-8703-4.00010-9

[10] Texas Instruments, "LMP7721 3-Femtoampere Input Bias Current Precision Amplifier," Texas Instruments Incorporated, Texas, USA, LMP7721 datasheet, Dec. 2008 [Revised Sept. 2014]. https://www.ti.com/document-viewer/LMP7721/datasheet

[11] W. Kester, J. Bryant, and M. Byrne, "Grounding Data Converters and Solving the Mystery of 'AGND' and 'DGND'," Analog Devices, Norwood, Massachusetts, Rep. MT-031, Oct. 2008.

[12] National Instruments, "NI 9239, " NI 9239 datasheet, Cary, NC, USA, Apr. 2016.

[13] *Model 6220 DC Current Source Model 6221 AC and DC Current Source Reference Manual*, Keithley Instruments, Cleveland, Ohio, USA, Rep. 622X-901-01, Jun. 2005. https://download.tek.com/manual/622x-901-01(B-Jun2005)(Ref).pdf

[14] J. O. Smith, "Welch's Method," in Spectral Audio Signal Processing, 2011, https://ccrma.stanford.edu/~jos/sasp/Welch_s_Method.html

[15] Stanford Research Systems, "Low-Noise Current Preamplifier," San Jose, California, USA, SR570 datasheet, https://www.thinksrs.com/downloads/pdfs/catalog/SR570c.pdf

[16] Keysight Technologies, "B2980A Series Femto/ Picoammeter and Electrometer / High Resistance Meter," MD, USA, B2981A datasheet, Aug. 2020, https://nscainc.com/wp-content/uploads/2020/12/NSCA-B2980A-Series-Femto-Picoammeter-and-Electrometer-High-Resistance-Meter-Datasheet-5991-4878.pdf